Adaptive-Scale Robust Estimator using Distribution Model Fitting

Thanh Trung Ngo[1], Hajime Nagahara[1], Ryusuke Sagawa[1], Yasuhiro
Mukaigawa[1], Masahiko Yachida[2], and Yasushi Yagi[1]

[1] Osaka University
[2] Osaka Institute of Technology

Abstract. We propose a new robust estimator for parameter estimation
in highly noisy data with multiple structures and without prior informa-
tion on the noise scale of inliers. This is a diagnostic method that uses
random sampling like RANSAC, but adaptively estimates the inlier scale
using a novel adaptive scale estimator. The residual distribution model
of inliers is assumed known, such as a Gaussian distribution. Given a
putative solution, our inlier scale estimator attempts to extract a dis-
tribution for the inliers from the distribution of all residuals. This is
done by globally searching a partition of the total distribution that best
fits the Gaussian distribution. Then, the density of the residuals of es-
timated inliers is used as the score in the objective function to evaluate
the putative solution. The output of the estimator is the best solution
that gives the highest score. Experiments with various simulations and
real data for line fitting and fundamental matrix estimation are carried
out to validate our algorithm, which performs better than several of the
latest robust estimators.

1 Introduction

Robust parameter estimation is fundamental research in the fields of statistics
and computer vision. It can be applied in many estimation problems, such as
extracting geometric models in intensity images and range images, estimating
motion between consecutive image frames in a video sequence, matching images
to find their similarity, and so on. In these problems, the data contains explana-
tory data, which also includes leverage elements, and a large number of outliers.
The data may also contain several structures, such as various lines or planes
that appear in pictures or range images of a building. Therefore, the common
requirements for a modern robust estimator in computer vision are: robustness
to various high outlier rates (high breakdown point [1]), ability to work with
multi-structural data and good detection of inliers.

In this paper, we present a new robust estimator that has a high breakdown
point, can work with multi-structural data and estimates the correct inlier scale.
Our method relies on a novel inlier scale estimator and a density-based objective
function. The proposed inlier scale estimator finds the most Gaussian-like parti-
tion globally in the residual distribution of a putative solution. This is the main

contribution of our paper. Since we find the best inlier scale for inliers globally, smoothness of the probability density is not strictly required, and therefore, we have chosen the histogram method for fast computation.

2   Related Works

Least median squares (LMS) [1] is the most well-known robust estimator in statistics and computer vision, and can achieve a high breakdown point [1] of up to 50% of the outliers. However, in a real estimation problem, such as extracting lines from an intensity image or extracting planes from a range image, where the outlier rate is higher than 50%, the LMS cannot be used. Some estimators, however, have a higher breakdown point than 50%. The RANSAC algorithm [9] and Hough transform [10] are the most popular in this regard. If the scale of inliers is supplied, RANSAC can reach a very high breakdown point. However, the drawback of RANSAC is that it needs a user-defined threshold to distinguish inliers. The Hough transform can also achieve a very high breakdown point if it is able to manage its large voting space. Certain extensions of the LMS, such as MUSE (minimum unbiased scale estimate) [2] or ALKS (adaptive least kth order squares) [3], can be applied with high outlier rates, but these have a problem with extreme cases, such as perpendicular planes, and are sensitive to small pseudo structures. Another extension of the LMS is MINPRAN (minimize probability of randomness) [4], which requires an assumption of the outlier distribution. This assumption seems to be strict since outlier distribution is assumed with difficulty. RESC (residual consensus) [5] computes a histogram of residuals and uses several parameters to compress the histogram. The histogram power is computed as the score for the putative estimate. RESC is claimed to tolerate single structure data that contains up to 80% outliers, however, it needs many user-defined parameters to compress the histogram and to detect the inlier distribution, which reduces its adaptiveness. The pbM (projection-based M-Estimator) [6][11] is an extension of the M-Estimator that uses projection pursuit and the KDE (kernel density estimation), and can provide a breakdown point greater than 50%. However, it only works for linear residual functions, such as linear regression, or linearized residual functions. Another robust estimator that uses the KDE is the ASSC (adaptive scale sample consensus) [7]. ASSC assumes that the inliers are located within some special structure of the density distribution; practically it detects the first peak from zero and the valley next to the peak to locate the inliers. ASSC can provide a very high breakdown point, around 80%, when the correct bandwidth for the KDE is applied. ASSC has subsequently been improved, resulting in ASKC (adaptive scale kernel consensus) [8], which has an improved objective function and higher robustness in the case of high outlier rates. The bandwidth for the KDE in ASKC is computed using a scale estimate that contains approximately 10% of the smallest residuals. However, this under-smoothed bandwidth causes the ASKC estimate to have very few inliers in the case of data with a low outlier rate, and this reduces the accuracy even though the breakdown point is still high. In contrast to the pbM, ASSC

or ASKC, our proposed method does not compute the inlier scale (the standard deviation of noise on the inlier residuals) directly from the estimated probability density. Since it roughly describes the true distribution and since the location of a local peak, global peak or local valley in the density estimation depends on a smoothing bandwidth, we find the best inlier scale globally by matching with a Gaussian distribution.

3 Adaptive-scale Robust Estimator

3.1 Problem Preliminaries

Assume the estimation of a structure model with the constraint:

$$g(\boldsymbol{\theta}, \boldsymbol{X}) = 0, \tag{1}$$

where $\boldsymbol{\theta}$ is the parameter vector of the structure, and $\boldsymbol{X}$ is an explanatory data point. Our estimation problem can then be described as follows.

- *Input*: N observed data points $\boldsymbol{X_i}, i = 1..N$, including both inliers and outliers.
- *Output*: Parameter $\boldsymbol{\theta}$ that describes the data.

In a real problem, each inlier $\boldsymbol{X^t}$ is affected by an unknown amount of noise. Therefore, the actual parameter $\boldsymbol{\theta}$ cannot be recovered, and some approximation of $\boldsymbol{\theta}$ needs to be estimated. In evaluating whether an approximate estimate $\hat{\boldsymbol{\theta}}$ is good or bad, the estimator can only rely on the statistics of the error for each data point. This error is called the residual, and is a non-negative measure in the proposed method. For each model estimation problem, there are numerous ways of defining the residual function, including using the original constraint function (1). Generally, however, the residual is defined as:

$$r_{\hat{\theta}} = f(\hat{\boldsymbol{\theta}}, \boldsymbol{X}). \tag{2}$$

The standard deviation of these inlier residuals is called the *"inlier scale"*, and is denoted by $\sigma_{\hat{\theta}}$. The problem is that $\sigma_{\hat{\theta}}$ is not known, and therefore, an inlier scale estimator tries to estimate it. This estimate is denoted by $\sigma_{\hat{\theta}}^*$. Once the inlier scale has been determined, the threshold $t_{\hat{\theta}} = \tau \sigma_{\hat{\theta}}^*$ can be decided to distinguish inliers from outliers.

Given an estimate $\hat{\boldsymbol{\theta}}$, and an inlier scale $\sigma_{\hat{\theta}}$, the probability density function is denoted as $P_{\hat{\theta}}(r)$. $P_{\hat{\theta}}(r)$ is normalized using the inlier scale $\sigma_{\hat{\theta}}$ and we denote this normalized density function as $P_{\hat{\theta}}^s(\frac{r}{\sigma_{\hat{\theta}}})$. As the estimate $\hat{\theta}$ approaches the correct value of $\boldsymbol{\theta}$, the distribution of inliers resembles more closely the ideal distribution. We call the ideal distribution when $\hat{\boldsymbol{\theta}} = \boldsymbol{\theta}$, the distribution model. The density function for the standardized distribution model, with a sample deviation of 1, is denoted as $G(\xi)$, $\xi \geq 0$. In this case, the standardized distribution model is the standard Gaussian distribution for the absolute of variables, denoted by AGD and described in Fig.1.

The proposed estimator works with data with multiple structures, and therefore, the residual distribution $P_{\hat{\theta}}(r)$ has multiple modes. The mode near the origin is assumed to belong to the inlier structure, while the others belong to the outlier structures. Therefore, we cannot use the whole distribution model $G(\xi)$ with $0 \leq \xi < \infty$ for matching. Only the portion of $G(\xi)$ with $0 \leq \xi \leq \kappa$ is assumed as the inlier distribution model and is used for matching. κ is selected so that the range $0 \leq \xi \leq \kappa$ contains more than 95% of the population; in this study, for example, we use $\kappa = 2.5$.

3.2 Proposed Robust Estimator

In most previous works, the authors have assumed that the inlier residual distribution is a Gaussian distribution. This is also true for our research. We propose an estimator that uses distribution matching to find the best inlier scale from the distribution of all residuals.

Inlier Scale Estimation by Matching the Residual Distribution to the Distribution Model The inlier scale is estimated by searching for the best fit between a segment of the residual distribution and the AGD. The segment of the residual distribution used for matching starts from zero. Then, the residual scale of the first structure is detected regardless of the outlier structures. The matching error between the density function $P_{\hat{\theta}}^s(\frac{r_{\hat{\theta}}^i}{\sigma})$ with assumed inlier scale σ and the AGD density function $G(\frac{r_{\hat{\theta}}^i}{\sigma})$ is defined by a simple minimization:

$$e_{\hat{\theta}}(\sigma) = \min_{k} \underset{0 \leq r_{\hat{\theta}}^i \leq \kappa\sigma}{Average}\{(P_{\hat{\theta}}^s(\frac{r_{\hat{\theta}}^i}{\sigma}) - kG(\frac{r_{\hat{\theta}}^i}{\sigma}))^2\}, \tag{3}$$

where k is some scale of the AGD density function, $r_{\hat{\theta}}^i$ is the ith residual and κ indicates the portion of the AGD used in the matching. Then, the best scale of inlier residuals $\sigma_{\hat{\theta}}^*$ is estimated by searching the scale that gives the smallest matching error. This is summarized as

$$\sigma_{\hat{\theta}}^* = \underset{\sigma}{argmin}\{e_{\hat{\theta}}(\sigma)\}. \tag{4}$$

Inliers are then distinguished using the threshold $t_{\hat{\theta}} = \kappa\sigma_{\hat{\theta}}^*$.

In our algorithm, to compute the probability density of the residual from an estimate $\hat{\theta}$, we apply the well-known histogram method, although the KDE can also be used. A histogram is simple and as residual sorting is not required, in contrast to most previous estimators, it gives a very low computational cost. Searching for the best inlier scale $\sigma_{\hat{\theta}}^*$ is graphically depicted in Fig.1.

Bin-width for the histogram is selected in the same way as in previous works [7][8]. A widely used bin-width [13] for robust estimators is:

$$\hat{b}_{\hat{\theta}} = (\frac{243 \int_{-1}^{1} K(\zeta)^2 d\zeta}{35N(\int_{-1}^{1} \zeta^2 K(\zeta)d\zeta)^2})^{\frac{1}{5}} \hat{s}_{\hat{\theta}}, \tag{5}$$
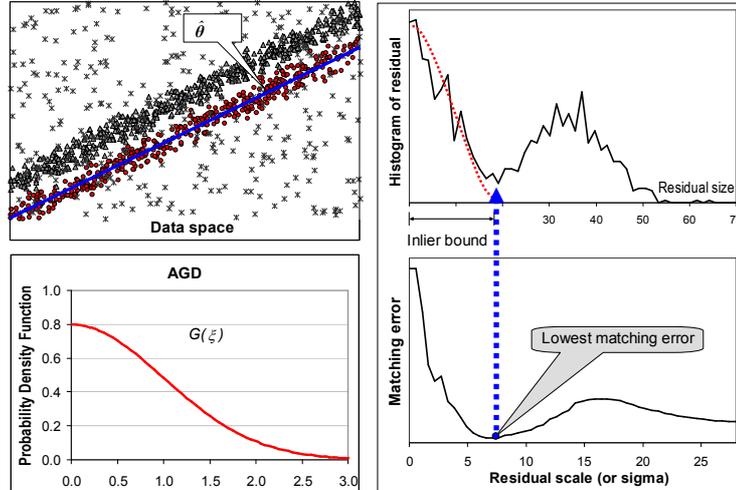
Fig. 1. Demonstration of searching the inliers scale. Data contains two actual parallel lines. The inlier scale is obtained by finding the smallest matching error.

where K is some kernel, such as the popular Gaussian kernel or Epanechnikov kernel, and $\hat{s}_{\hat{\theta}}$ is the smallest window containing 15% of the smallest residuals.

Objective Function Inspired by the use of the KDE in the pbM-Estimator [11] and ASKC [8], we also apply it in our adaptive objective function:

$$F(\hat{\boldsymbol{\theta}}) = \frac{1}{Nh_{\hat{\theta}}} \sum_{i=1}^{N} K(\frac{r_{i,\hat{\theta}}}{h_{\hat{\theta}}}), \qquad (6)$$

where $h_{\hat{\theta}}$ is adaptively estimated and K is a kernel such as the Gaussian kernel K_G or Epanechnikov kernel K_E. The KDE objective function evaluates how densely the residuals are distributed at zero using the kernel's window. In our case, the window of kernel K is $h_{\hat{\theta}}$, which tightly fits the estimated inliers, and therefore, the objective function gives the density measured at zero for the estimated inliers only. For K_G, $h_{\hat{\theta}} = \hat{\sigma}_{\hat{\theta}}^*$ and for K_E, $h_{\hat{\theta}} = \kappa \hat{\sigma}_{\hat{\theta}}^*$.

3.3 Estimation Algorithm Summary

We summarize the proposed algorithm below.

(a) Create a random sample and then estimate the solution parameters $\hat{\boldsymbol{\theta}}$.
(b) Estimate all the residuals of the data points given the parameters $\hat{\boldsymbol{\theta}}$.
(c) Estimate the bin-width by (5), and then compute histogram $P_{\hat{\theta}}$.
(d) Estimate the inlier scale as summarized by (4).
(e) Estimate the score using the objective function (6).
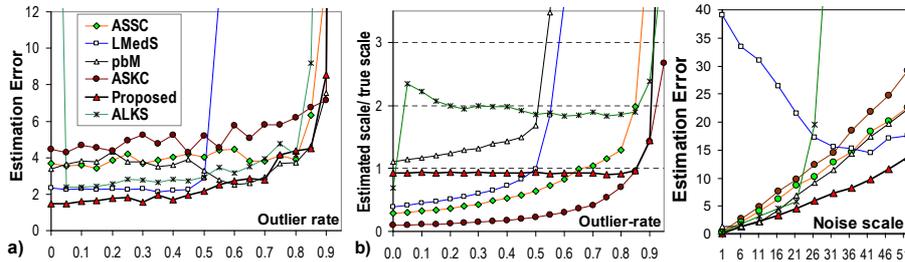(f) Update the best solution.
(g) Repeat from (a) if not terminated.

Fig. 2. Experiment on outlier rates

Fig. 3. Experiment on noise scales

4 Experiments

We carried out several experiments to validate our algorithm in linear and non-linear estimation problems: plane fitting, line fitting and fundamental matrix estimation. First, we used a simulation to understand the various aspects of the algorithm, and then actual experiments were performed with real data to validate the algorithm in various real situations. For the plane and line fitting (linear residual) problems, we compared our algorithm with several popular robust estimators: the pbM, LMedS, ALKS, ASSC, and ASKC. For the fundamental matrix (using non-linear residual) estimation, we used LMedS, ASSC, ASKC, and ALKS for comparison, since the pbM was originally proposed for linear robust regression problems. ALKS is very unstable when k is small, and therefore, in our experiments we only started searching for k when it was greater than 15% of the total number of data points. The Epanechnikov kernel was used in the KDE as well as the related objective functions. All algorithms were supplied with the same set of random sampling hypotheses and no optimization. For the proposed estimator, κ was selected such that the portion of the AGD for matching contained about 97% of the population; $\kappa = 2.5$ was used for all the experiments. The following criteria were used for validating the proposed estimator:

- Robustness through various outlier rates and noise scales.
- The ability to work with data with multiple structures.

4.1 Linear Fitting

In this problem, the estimator must extract the correct line or plane from a dataset that contains single or multiple structures with the appearance of random outliers. The experiments were carried out using various popular analytic simulations for the robust estimator. Given an estimate $\hat{\boldsymbol{\theta}} = (\hat{a}, \hat{b}, \hat{c}, \hat{d})$, the estimation error is defined as:

$$Error_{\hat{\theta}} = \sqrt{(a - \hat{a})^2 + (b - \hat{b})^2 + (c - \hat{c})^2 + (d - \hat{d})^2}, \qquad (7)$$

where (a, b, c, d) are ground-truth parameters. The normal vector of each plane is normalized such that $\sqrt{a^2 + b^2 + c^2} = 1$, $\sqrt{\hat{a}^2 + \hat{b}^2 + \hat{c}^2} = 1$.
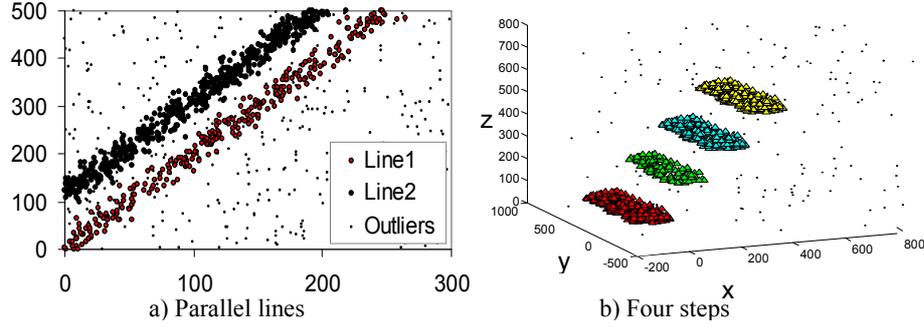
Fig. 4. Multiple data examples: (a) parallel lines and (b) data with 3D steps

Single Structure with Various Outlier Rates: We simulated a random dataset containing a random 3D plane with 500 random points within a 3D volume [0, 0, 0, 1000, 1000, 1000]. Some of the inlier points were replaced by outliers with random coordinates, thereby keeping the total number of data points as 500. The inlier points were contaminated by Gaussian noise with scale $\sigma_G=8$. The average results for 100 such datasets are shown in Fig.2. Fig.2(a) shows the estimation errors for robust estimators and Fig.2(b) shows the ratio between the estimated inlier scale and the actual inlier scale. The proposed estimators, pbM, ASSC and ASKC, have similar breakdown points, and they can work with very high outlier rates, up to 90%. However, with regards accuracy of the estimation and estimated inlier scale, the proposed estimator gives the best results. The estimated inlier scale is close to the actual inlier scale, with the ratio between them almost 1.

Single Structure with Noise Levels on Inliers: The dataset was set up in the same way as in Section 4.1 for line fitting, but the outlier rate was fixed at 60%, and the noise scale σ_G varied between 1 and 52. The average results for 100 datasets are shown in Fig.3. These results show that the performance of each estimator decreased as the noise scale increased. However, the proposed estimator was highly resistant to the high noise scale.

Parallel Lines with Varying Distances: This problem demonstrates the ability of line estimation with the appearance of multiple structures. A dataset containing two parallel lines is used in this experiment. The estimator must then discriminate the two lines and extract a line correctly from the data. The experiment was carried out with varying distances between the two parallel lines:

$$Line1 : 2x - y + d = 0, \; where \; d = 20, 30, 40, ...210$$
$$Line2 : 2x - y \quad = 0.$$

Each dataset contained 450 random points (outliers); 150 points on $line1$ and 300 points on $line2$ were generated randomly for each trial in this experiment.
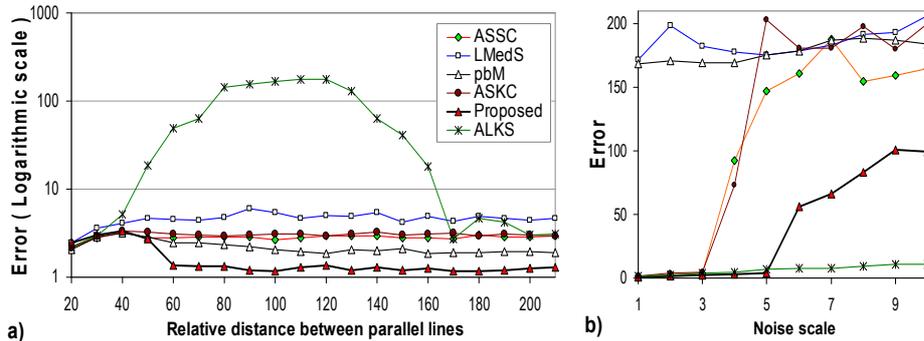
Fig. 5. Estimation errors for data (a) with parallel lines and (b) with steps

Gaussian noise with a zero mean and σ_G=8.0 was added to the points on each line, whilst keeping the range of all points within the rectangle (0, 0, 62.5σ_G, 62.5σ_G). An example of a random dataset is shown in Fig.4(a) with $d = 80$. The average results from 100 trials for the estimation error and number of estimated inliers are shown in Fig.5(a). When the two lines are close together, $d = 20$, they are almost mistaken for one line, with all estimators having a similar accuracy. When the lines are further apart, the performance of ALKS is the worst, as it only manages to estimate correctly once the two lines are very far apart. Since the actual outlier rate for estimating any line is greater than 50%, LMedS produces worse results as the two lines move further apart. However, our proposed algorithm retains a similar accuracy rate irrespective of the distance between the lines. The pbM, ASSC and ASKC have the same robustness as the proposed estimator, but with lower accuracy.

Multiple Steps with Varying Noise Levels: In this experiment, step data consisting of four planes was set up as shown in Fig.4(b). The parameters of the actual planes are:

$$Plane\ 1 : z - 100 = 0$$
$$Plane\ 2 : z - 200 = 0$$
$$Plane\ 3 : z - 300 = 0$$
$$Plane\ 4 : z - 400 = 0$$

The dataset for evaluation consisted of 240 random points for each plane and 240 random outliers. Each data point on a plane was contaminated by Gaussian noise with σ_G. The experiment was carried out to test all the estimators with different values of σ_G. With larger values of σ_G, the four planes are closer and may become fused. The results are illustrated in Fig.5(b), which gives the average of the results for 100 such randomly generated datasets.

The pbM did not perform well in this experiment as it mistook the four planes for the same structure, resulting in the estimated number of inliers being about four times more than the actual number of inliers for each plane. LMedS

did not perform well either, as the outlier rate is high for the estimation of any plane. ASSC and ASKC were able to estimate correctly only at low noise levels. The proposed method was able to function correctly at slightly higher noise levels, but then it also became confused and estimated the four planes as a single plane. Since ALKS is well known for its instability and sensitivity to small pseudo structures, we limited the size of possible structures for ALKS, with the estimated structure being larger than 15% of the data. Hence, ALKS was able to function at much higher noise levels. In this case its sensitivity was an advantage.

4.2 Fundamental Matrix Estimation in Real Video Sequences
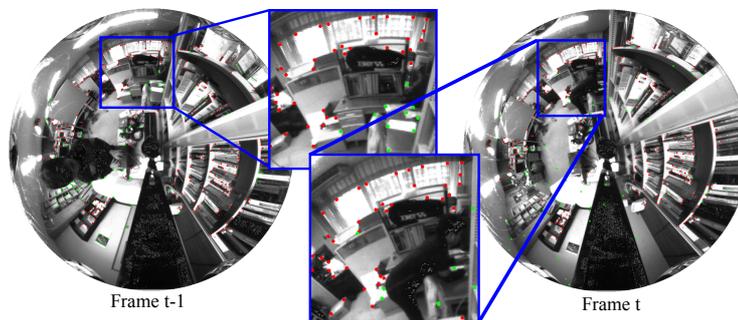

Frame t-1

Frame t

Fig. 6. One pair of images in a sequence; inliers (image features in red) and outliers (image features in green) are output by the proposed estimator

In these experiments, real video sequences were captured in an indoor environment with an omnidirectional vision sensor. Examples of the captured images are shown in Fig.6. The sensor consisted of an omnidirectional mirror, a telecentric lens and an imaging sensor. The camera was mounted on a rotary stage and controlled by a PC, which translated the camera whilst it was being rotated. For each pair of images, 200 Harris image features were detected on the first image and tracked on the second image to obtain the feature correspondence pairs using the KLT feature tracker [12] implemented in OpenCV. The fundamental matrix between a pair of consecutive images was computed using the seven point algorithm [16] with these feature correspondence pairs. The residual function is defined in [15]:

$$
r = f(\boldsymbol{F}, \boldsymbol{x}, \boldsymbol{x}') = \left| \boldsymbol{x}'^{\boldsymbol{T}} \boldsymbol{F} \boldsymbol{x} \right| \sqrt{\frac{1}{\parallel \boldsymbol{F} \boldsymbol{x} \parallel^2} + \frac{1}{\parallel \boldsymbol{F}^T \boldsymbol{x}' \parallel^2}}, \tag{8}
$$

where F is the fundamental matrix and $(\boldsymbol{x}, \boldsymbol{x}')$ a feature correspondence pair. Since we cannot compare the estimated fundamental matrix with a ground-truth fundamental matrix, we compute the error as the standard deviation of

only inlier residuals of the estimated fundamental matrix $\hat{\boldsymbol{\theta}}^* = \hat{\boldsymbol{F}}^*$:

$$Error_{\hat{\boldsymbol{F}}^*} = \sqrt{\frac{1}{M} \sum_{i=1}^{M} (r_{i,\hat{\boldsymbol{F}}^*})^2}, \qquad (9)$$

where M is the number of inliers. This error computation relies on how the solution fits the motion data: a better fit produces smaller residuals for inliers, and vice versa. In a simulation, the actual inliers are known and thus M is known. In a real experiment, the error is computed for the M smallest residuals (which are considered inliers), with M assigned manually after checking the actual data.

For each video sequence, about 50 images were captured, whilst ensuring the same rotation between consecutive images. The performance of all the estimators tends to deteriorate with a greater degree of rotation, since the KLT tracker is less accurate under greater rotation. Therefore, we used three video sequences with different rotation settings. These video sequences are referred to as $Video\_4deg$, $Video\_14deg$ and $Video\_18deg$ for rotation speeds of 4 degrees/frame, 14 degrees/frame, and 18 degrees/frame, respectively. We computed the error by (9) and M was set independently for each video sequence after randomly checking five pairs of images within each video sequence. The average number of true inliers and the assigned value for M for each video sequence are given in Table.1. The average errors and number of estimated inliers for 100 executions of each video sequence are given in Table.1. For low outlier rates, LMedS gave the best accuracy. However, for a high outlier rate in $Video\_18deg$, LMedS performed worst. The estimation error of the proposed method is quite similar to that of ASSC. With regard to the number of estimated inliers, the proposed method gave the best results, the number of estimated inliers was close to the actual number of inliers.

Table 1. Fundamental matrix estimation error and number of estimated inliers for real video sequences

Video sequence	Video_4deg		Video_14deg		Video_18deg	
Number of true inliers	187.7		102.7		72.2	
Assigned M	160		90		60	
Fitting error / No est. inliers						
Proposed method	0.00152	150.7	0.00377	86.4	0.00382	65.5
ASSC	0.00156	36.7	0.00377	38.7	0.00385	39.9
ASKC	0.00184	22.7	0.00474	23.6	0.00507	23.9
ALKS	0.00903	66.8	0.01955	98.7	0.02127	64.5
LMedS	0.00125	101.0	0.00349	101.0	0.00574	101.0

Fig.7 shows the estimated distributions of residuals (from both inliers and outliers) for the estimators with the sequence $Video\_18deg$. For each estimator, the distribution was computed as the average of the residual distributions for the solutions for all pairs of images. The graph shows that the distributions and the Gaussian are highly correlated regardless of the estimator.
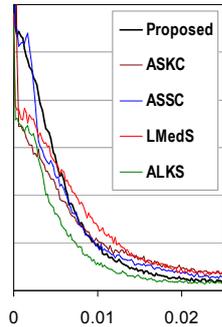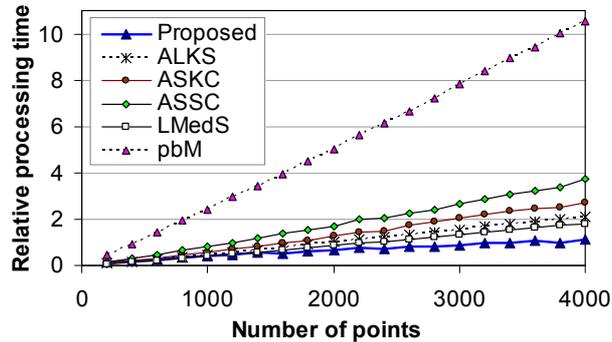
Fig. 7. Actual distribution of residuals

Fig. 8. Processing time for all estimators

4.3 Computational cost

We simulated the relation between processing time and the number of data points, the average results of which are shown in Fig.8. In this simulation, a linear fitting problem for a plane was used and all the estimators were given the same set of random samples. The graph shows that overall the proposed estimator gives the fastest computational time, especially for large data.

5 Discussion and Conclusions

In this paper, we proposed a novel highly robust estimator for the estimation problem in computer vision that deals with data with high outlier rates and multiple structures. Our algorithm does not need any prior information about the inlier scale, as this is estimated adaptively by globally searching for the best match of the Gaussian distribution and the residual distribution. Thus, the inlier residual distribution is tightly estimated, resulting in robustness and high accuracy for the proposed algorithm. The validity of the proposed algorithm was confirmed by experiments with several different estimation problems in various situations.

Without a smoothing parameter, such as bin-width in the proposed estimator and bandwidth in ASSC, the residual statistics are unstable, especially for a small set of residuals. This reduces the robustness of an adaptive robust estimator, as is the case in ALKS. ALKS tends to extract smaller structures that have a distribution similar to the Gaussian distribution. However, in a small set of residuals, this distribution is likely to occur. Using a smoothing parameter in the residual density estimation can make an adaptive-scale estimator more robust, as is the case in ASSC, ASKC, and pbM. However, the problem lies in how large this parameter should be. For example, in ASSC and ASKC, the estimated inlier scale is correlated with the bandwidth but not with the actual outlier rate. The inlier scale is frequently underestimated for data with low outlier rates. The proposed estimator is designed to estimate the inlier distribution tightly, and

therefore the inlier scale is always close to the actual inlier scale regardless of the outlier rate.

In current method, we assume the Gaussian distribution for inlier residuals. In future, we would like to improve the algorithm for application to distribution models other than the Gaussian.

References

1. P.J. Rousseeuw and A. Leroy. Robust Regression and Outlier Detection. John Wiley & Sons, New York. 1987.
2. J.V. Miller and C.V. Stewart, MUSE: Robust surface fitting using unbiased scale estimates, Proc. of CVPR, pp. 300–306, 1996.
3. K.M. Lee, P. Meer, and R.H. Park, Robust adaptive segmentation of range images, TPAMI, Vol.20, pp. 200–205, 1998.
4. C. V. Stewart, MINPRAN: A new robust estimator for computer vision, TPAMI, Vol.17, pp. 925–938, 1995.
5. X. Yu, T.D. Bui, A. Krzyzak, "Robust Estimation for Range Image Segmentation and Reconstruction," TPAMI, vol. 16, no. 5, pp. 530-538, May, 1994.
6. H. Chen and P. Meer, Robust regression with projection based M-estimators, ICCV, pp. 878-885, 2003.
7. H. Wang and D. Suter, Robust Adaptive-Scale Parametric Model Estimation for Computer Vision, IEEE TPAMI, Vol.26, No.11, pp. 1459–1474, 2004.
8. H. Wang, D. Mirota, M. Ishii, G.D. Hager, Robust Motion Estimation and Structure Recovery from Endoscopic Image Sequences With an Adaptive Scale Kernel Consensus Estimator, CVPR 2008.
9. M. A. Fischler and R. C. Bolles, Random Sample Consensus: A Paradigm for Model Fitting with Applications to Image Analysis and Automated Cartography, Comm. of the ACM 24, pp. 381–395, 1981.
10. J. Illingworth and J. Kittler, A survey of the Hough transform, Computer Vision, Graphics, and Image Processing (CVGIP), Vol.44, pp. 87–116, 1988.
11. R. Subbarao, P. Meer, Beyond RANSAC: User Independent Robust Regression, p. 101, CVPRW 2006.
12. J. Shi and C. Tomasi, Good Features to Track, Proc. of IEEE CVPR, pp. 593–600, 1994.
13. M.P. Wand and M. Jones. Kernel Smoothing. Chapman & Hall. 1995.
14. R. Subbarao, P. Meer, pbM-Estimator source code, http://www.caip.rutgers.edu/riul/research/robust.html
15. Q.T. Luong and O.D.Faugeras, The fundamental matrix: Theory, algorithms, and stability analysis, Intl. Journal of Computer Vision, Vol.17, No.1, pp. 43–75, 1996.
16. R.I. Hartley, Projective reconstruction and invariants from multiple images, IEEE Trans. on Pattern Analysis and Machine Intelligence, Vol. 16 (10), pp.1036–1041, Oct 1994.